# Effect of Aging on Material Properties and Partial Discharge Characteristics of Insulating Pressboard

Yongqiang Wang,* Xia Zhang, Xiaolei Jiang, and Yunjia Wang

Pressboard samples with different aging degrees were prepared to study the material and discharge characteristics of pressboards with a shielding electrode. The step-up method was used for the subsequent experiment. The partial discharges of the pressboards with different aging degrees were compared and combined using Fourier transform infrared spectra, as well as electric field simulations and analysis. The microstructure of the aged pressboards was observed with scanning electron microscopy. The results showed that pre-discharge occurred mainly in the oil gap between the hemispherical electrode edge and pressboard. Aging the pressboard had no obvious effect on the discharge characteristics at the initial partial discharge stage. As the partial discharge developed, aging the pressboard resulted in a higher electric field intensity acting over a greater area, which led to a more intense discharge. Microscopic observation showed that aging and discharge destroyed the fibre, reduced the fibre width, and caused holes and fractures, which promoted further development of the discharge. The spectroscopic analysis showed that aging destroyed O-H functional groups and reduced the intermolecular forces and mechanical properties of the pressboard.

*Keywords: Insulating pressboard; Surface discharge; Thermal aging degree; Shielding electrode; Electric field; Scanning electron microscope; Fourier transform infrared spectra*

*Contact information: Hebei Provincial Key Laboratory of Power Transmission Equipment Security, Department of Electrical Engineering, North China Electric Power University, Baoding 071003, China;*
** Corresponding author: qianghd@126.com*

## INTRODUCTION

A transformer bushing is an important component in lead insulation. The end of a high-voltage bushing is often equipped with a shielding electrode to ensure a uniform electric field (Zhang *et al.* 2012; Wang *et al.* 2015; Zhang *et al.* 2017). However, the distribution of the electric field on the surface of the shielding electrode is not uniform, and the partial discharge (PD) of oil-paper insulation in areas of local high electric field intensity occurs readily and develops into surface discharge. Therefore, the insulation of a high-voltage bushing is in fact a weakness in the insulation of a transformer and it is necessary to study the aging behaviour and PD characteristics of the insulating pressboard.

Oil-paper insulation is the main form of internal insulation in power transformers (Harbaji *et al.* 2015; Xia and Wu 2016; Chen *et al.* 2017; Hao *et al.* 2018). There is much research available on the aging of oil-paper insulation and the factors that affect PD (Zhou *et al.* 2015; Wei *et al.* 2016a; Xie *et al.* 2016a; Sun *et al.* 2017; Munajad *et al.* 2018). Mitchinson *et al.* (2008) designed a model for point discharge and investigated the effects of voltage and time on oil-paper insulation. The influence of aging the pressboard and oil on the surface discharge was studied for four oil/pressboard specimens with different aging degrees, and the characteristics of PD from inception to flashover have also been studied

(Li *et al.* 2009). Xie *et al.* (2016b) combined the PD information pertaining to pressboards with different aging degrees, using simulations to investigate the effect of pressboard aging on the development of the surface discharge.

Presently, most of the electrodes in the surface discharge model of oil-paper insulation are parallel plate or column plate electrodes. However, reports on modelling of the shielding electrode at the end of a high voltage bushing are rare. Therefore, the shielding electrode was simplified and a hemispherical electrode was designed for the present experimental work to observe the surface characteristics of pressboards and development of the surface discharge. The insulation pressboard samples with different aging degrees were prepared with accelerated thermal aging. These experiments allowed information about the PD to be collected, and then according to electric field simulation of the pressboard, scanning electron microscope (SEM) images and Fourier transform infrared (FTIR) images, the discharge characteristics of insulating pressboards were summarised.

## EXPERIMENTAL

### Experimental Model and Platform Design

A hemispherical copper electrode was designed (Fig. 1). Figures 1a and 1b are the front view and side view of the structure model, respectively. Figure 1c is the physical map of the hemispherical model. The upper electrode was hemispherical with a diameter of 40 mm and the lower electrode is a prism measuring 40 mm × 40 mm × 120 mm. The insulating pressboard in the middle of the two electrodes measured 80 mm × 80 mm × 2 mm. The experimental platform is shown in Fig. 2.

The pulse current method was used to detect the PD signals. The oil-immersed transformer was a YDTW 50/250 (Jiangdu Huayu High Pressure Electric Co., Ltd., Yangzhou, China). The ratio of the voltage divider was 1500:1, and the divided voltage signal and partial discharge signal were sent to the HCPD-2022-type portable PD tester (Baoding Huachuang Dianqi Development Co. Ltd., Baoding, China) for processing. Its sampling frequency was set to 20 MHz, and the protection resistance was 10 kΩ.

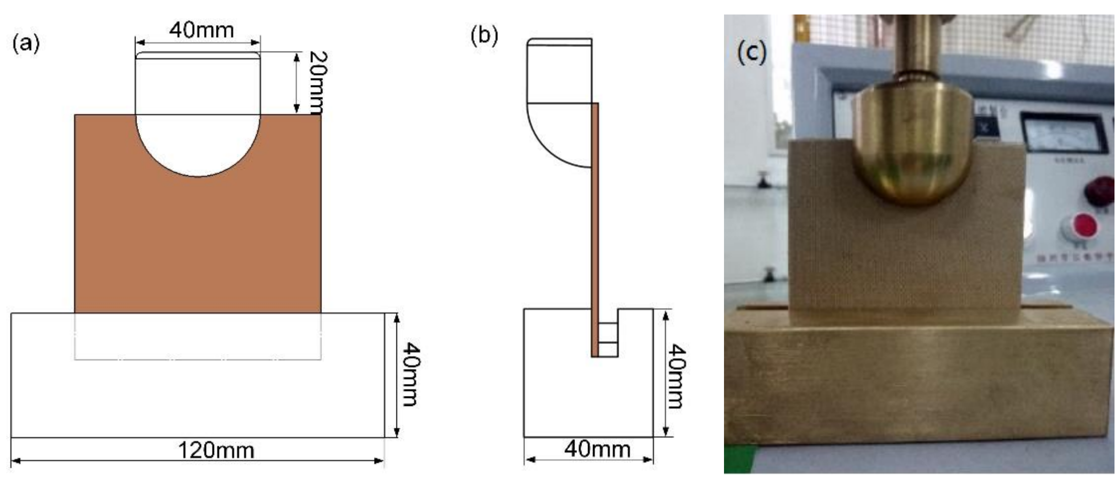


**Fig. 1.** Hemispherical discharge model: (a) structure model positive graph, (b) structure model side graph, and (c) hemispherical model

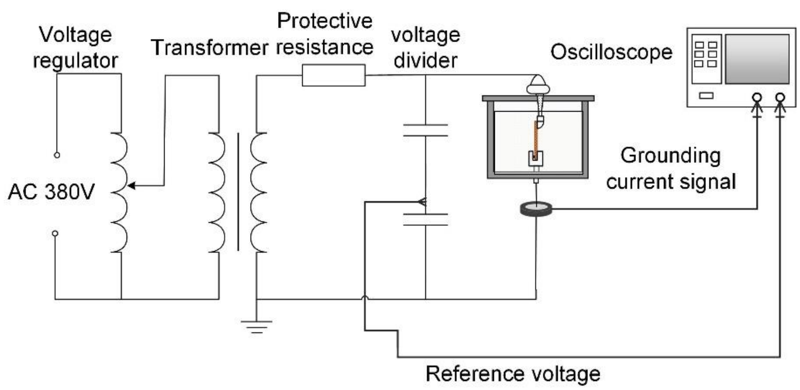


**Fig. 2.** Schematic diagram of the experimental platform

## Preparation of the Experimental Samples

The experiment employed the widely-used No. 25-grade transformer oil, and insulating pressboard was made from ultra-high voltage transformer pressboard with a thickness of 2 mm (Weidmann Company, Switzerland). The test samples were pre-treated by first filtering the oil sample, and then the samples were left to stand for 24 h. The pressboards were dried in a vacuum drying oven at 120 °C under a pressure of 50 Pa for 24 h. The processed pressboards were impregnated with the treated oil sample in a sealed vacuum container for 48 h.

According to previous research (Tobazcon 1994; Yang *et al.* 2016; Zou *et al.* 2016), the extent of thermal aging of insulation pressboard mainly depends on the temperature and time. The accelerated thermal aging method was used to process the pressboard, and the aging life was estimated according to the Montsinger rule. When the working temperature of the insulating pressboard is higher, the insulation life is shorter. To reduce the time taken for each experiment, it is necessary to increase the aging temperature. Also, the flash point of the No. 25 oil is 142 °C, so a temperature of 130 °C was chosen for this thermal aging process. The aging life is estimated according to the Montsinger rule (Tu *et al.* 2016; Zhou *et al.* 2017), as shown in Eq. 1,

$$T = Ae^{-\alpha(\theta-\theta_0)} \tag{1}$$

where $T$ is the insulation life at the accelerated thermal aging, $A$ represents insulation life at the standard operating temperature, $\theta$ is the temperature of accelerated thermal aging, the value of which is 130 °C, $\theta_0$ denotes the standard operating temperature, the value of which is 80 °C, and $\alpha$ is the heat aging coefficient, generally taken as 0.1155.

Considering the influence of copper on aging in actual transformer (Fofana *et al.* 2002; Liao *et al.* 2009), the volume ratio of the treated insulating pressboard, copper, and oil sample was 1:1:10. They were placed into a vacuum drying box and aged at 130 °C. According to the Montsinger rule, the aging periods were 8 d, 16 d, 32 d, and 48 d, which were deemed equivalent to a transformer service life of 7 years, 14 years, 28 years, and 42 years, respectively. After the pressboards were dried, the water content of the pressboards was 480 ppm, as measured using a colorimetric KF titrator (Type-C30S, Mettler Toledo, Switzerland). To reduce the influence of aging the oil, the pressboards were immersed in fresh oil after being treated in a sealed container before testing for 24 h. The process was repeated three times.

### Experimental Method

The step-up boost method was used to increase the voltage at a rate of 2 kV/30 s until a more stable PD signal was found, and that voltage was held for 10 min. If the discharge signal remained relatively stable, the voltage was recorded as the initial discharge voltage $U_0$. The voltage was increased to $1.2 \times U_0$ and increased by 2 kV for each set of 120 data points (approximately 10 min to 15 min) until flashover occurred along the surface. The aging degree of each group was applied to three groups of the pressboard samples. The discharge information at different voltages was recorded, and the average value was finally used for the subsequent analysis.

### Analysis methods

Following methods were adopted to better analyze the PD characteristics of insulating pressboards with different aging degrees.

In order to study the influence of different aging degree on electric field distribution, finite element software Comsol (COMSOL Inc., MA, USA) was used to establish a numerical model, to mesh, and to simulate the electrical field. The physical model was used to simulate a steady static electrical field. In addition, the electrodes used were made of copper material and the hemispherical electrode was supplied with a voltage of 40 kV, and the other electrode was set at a voltage of zero.

The SEM EM-30 PLUS made by COXEM (Daejeon, Korea) was used to magnify the carbonization trace on the surface of insulating pressboard, which scanned the surface fiber morphology of insulating paper at different aging degrees. Finally, the structure and quantity of functional groups in insulating paper at different discharge stages were analyzed by FTIR (Nicolet iS5, Thermo Fisher, Shanghai, China). The scanning frequency of FTIR was set to 32 times, the resolution of 4.0 $cm^{-1}$, and the wavenumber range used was 600 $cm^{-1}$ to 4000 $cm^{-1}$. The background air was scanned before each sample measurement to eliminate external interference. The final scanning result was displayed by absorbance.

## RESULTS AND DISCUSSION

### Initial Discharge and Flashover Voltages of the Pressboard

The initial PD and flashover voltages of the pressboard are listed in Table 1. The curve of initial discharge voltage with aging time is shown in Fig. 3. The initial discharge and flashover voltage underwent small decreases with an increase in the aging degree of the pressboard.

**Table 1.** Initial Discharge and Flashover Voltage of Insulating Pressboards

| Aging Time (d) | 8 | 16 | 32 | 48 |
|---|---|---|---|---|
| Initial Discharge Voltage (kV) | 30.5 | 30 | 29.3 | 28.5 |
| Flashover Voltage (kV) | 48 | 46 | 44 | 44 |

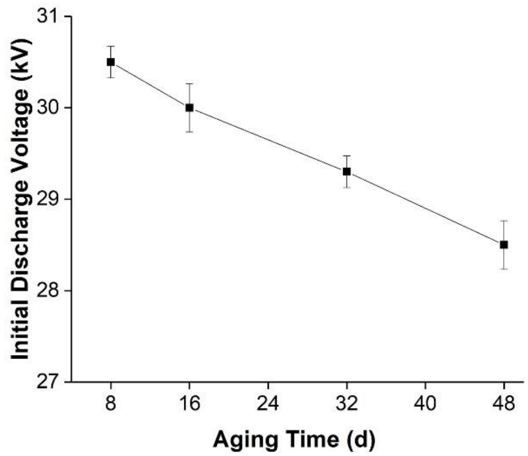


**Fig. 3.** Development of the initial discharge voltage

## Discharge Times of the Pressboard Samples

Figure 4 shows that the discharge times from the pressboard samples with different aging degrees increased with the voltage. The discharge times is the number of PD pulses under the corresponding voltage. In the late stage of discharge, the number of discharges was reduced to a certain extent. From 42 kV to 44 kV, the pressboard aged for 8 d showed a sharp decrease in the discharge times. After aging for 16 d, the discharge times increased slowly, but they decreased slightly between 44 kV and 46 kV. After aging for 32 d, the pressboard discharge times exhibited rapid growth, but remarkably decreased from 40 kV to 44 kV. After 48 d of aging, the starting discharge frequency was relatively high and the lowest frequency was found at 36 kV. Then, the discharge times gradually increased.

It was concluded that the hemispherical electrode pressboard discharge times increased with the voltage, but during the development of the discharge event, the discharge times at a certain voltage decreased, while the voltage decreased as the aging degree increased. At the same voltage, the discharge frequency increased upon aging.

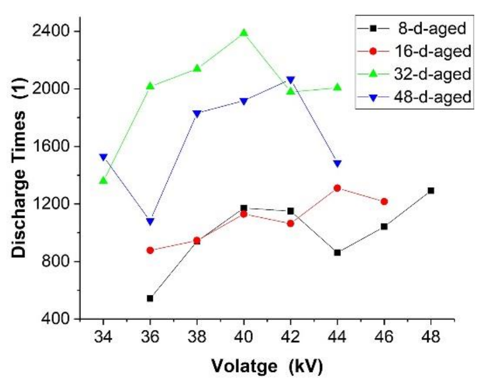


**Fig. 4.** Development of the discharge times

## Maximum PD Magnitude

Figure 5 illustrates that the maximum discharge magnitude changed with an applied voltage. The maximum discharge magnitude generally increased with the development of the discharge. The maximum PDs at different ages in the final stage of PD are as follows: after 8 d, 16 d, 32 d, and 48 d of aging, the maximum PDs were 9450 pC, 11326 pC, 13532 pC, and 24685 pC, respectively. The maximum PD increased upon aging.

In the early stage of discharge, the maximum discharge magnitude of the pressboard increased, albeit slowly, and the aging degree and maximum discharge magnitude were unrelated. During PD development and the later PD stage, the maximum discharge magnitude of the pressboard surface discharge increased rapidly. The growth curve was quasi-linear, and upon further aging, the maximum discharge magnitude increased at a faster rate.

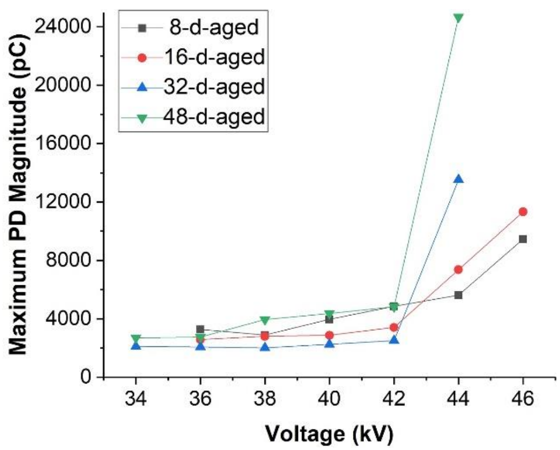


**Fig. 5.** Development of the maximum discharge magnitude

## Mean Discharge Magnitude

Figure 6 shows the change curve of the mean discharge magnitude with voltage. The mean discharge magnitude increased with the PD development, and the overall trend was similar to that of the maximum discharge. In the early stage of discharge, the mean discharge magnitude of the pressboard increased slowly. The mean discharge magnitude of pressboards aged 8 d, 16 d and 32 d had little difference, while that of the pressboard aged 48 d was lager. During PD development and the later PD stage, the mean discharge magnitude increased rapidly, similar to the maximum discharge magnitude, and the higher the aging degree of pressboard, the faster the mean discharge magnitude increased.

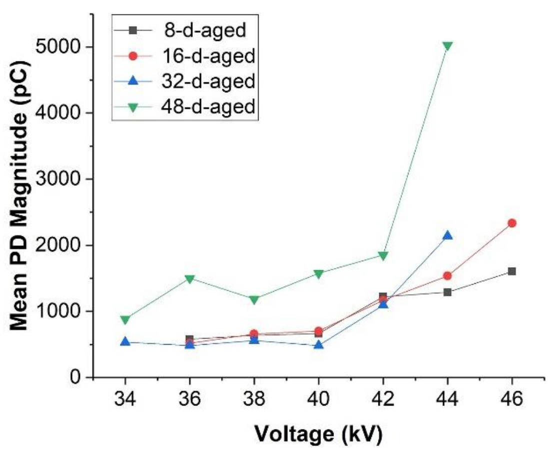


**Fig. 6.** Development of the mean discharge magnitude

## Phase Spectra of the Discharge Magnitude

The phase spectra of the discharge magnitude at different stages of PD are shown in Figs. 7 to 9. In the initial stage (Figs. 7a, 8a, and 9a), the discharge magnitude of the pressboard aged for 8 d and 32 d was between 0 pC and 5000 pC, and the distribution of the discharge magnitude was more uniform. The overall shape could be described as a half-slope or spire. The discharge magnitude of the 48-d-aged pressboard was more concentrated. The PD had a flat-topped shape in its first quadrant, was round from 200° to 290°, and had a spire shape from 180° to 355°. In the PD middle stage, the discharge phase became wider by between 5° and 10°, and the discharge times increased compared with that in the previous stage. The PD in each phase was denser, and the maximum discharge magnitude increased. In the PD later stage, the discharge phase of the three groups of the aged pressboard was wider, and the overall maximum discharge values were all near the first quadrant. The PD phase of the 8-d-aged pressboard was mainly concentrated in the 0° to 180° range and had a sloped shape. After aging for 32 d, the pressboard discharge phase was between 45° and 135°, which indicated a fault phenomenon. From 150° to 300°, the PD was intense and took on a half-slope shape. After aging for 48 d, the phases between 180° to 280° and 330° to 360° encompassed the most concentrated discharge magnitude. The discharge magnitude was between 0 pC and 8000 pC.

It was observed that the discharge phase of the pressboard under the hemispherical defect model was roughly divided into three ranges: 0° to 90°, 150° to 225°, and 330° to 360°. With the development of the event, the phase of the discharge gradually increased to 45° to 50°. Therefore, with the development of the PD, the discharge phase of the pressboard gradually widened. When aging was more severe, the mean discharge magnitude was higher. Meanwhile, the PD patterns of the different pressboard ages showed a broader discharge interval, and the maximum and mean discharge magnitudes increased with the aging degree.

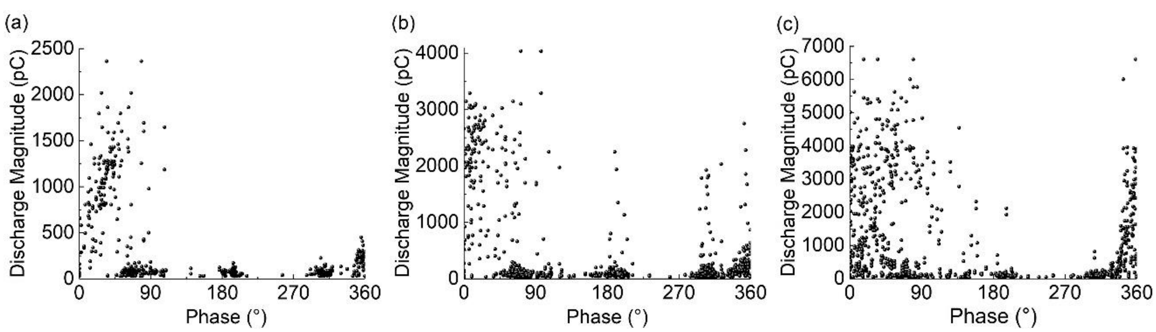


**Fig. 7.** PD patterns of the pressboard aged for 8 d: (a) initial PD stage, (b) PD middle stage, and (c) PD later stage

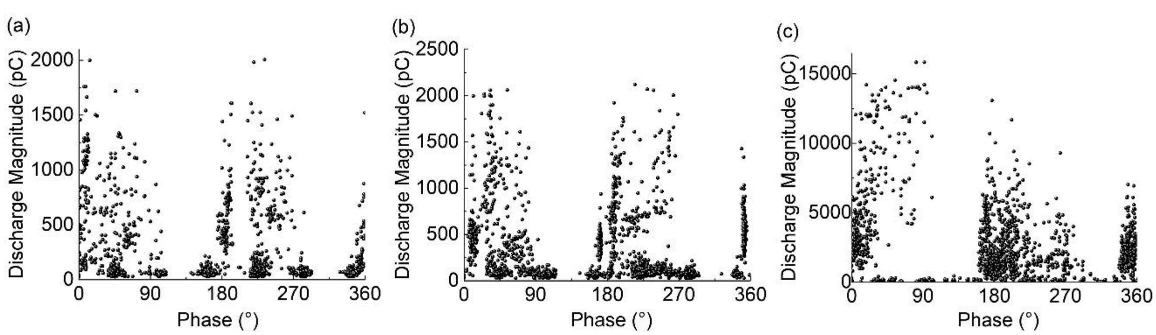


**Fig. 8.** PD patterns of the pressboard aged for 32 d: (a) initial PD stage, (b) PD middle stage, and (c) PD later stage

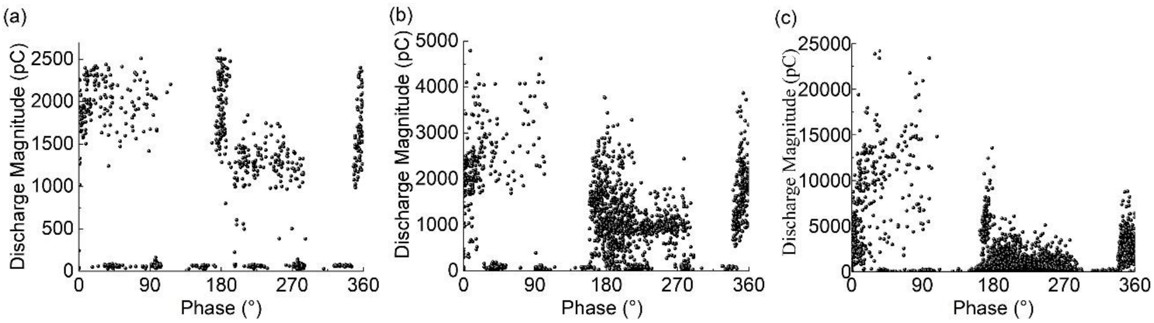


**Fig. 9.** PD patterns of the pressboard aged for 48 d: (a) initial PD stage, (b) PD middle stage, and (c) PD later stage

## Simulation and Analysis of the Electric Field

It was found that the internal porosity increased with an increased aging degree of the pressboard (Wei *et al.* 2016b; Zhou *et al.* 2016; Cui *et al.* 2017). To study the influence of aging on the PD of the pressboard, 1 bubble, 3 bubbles, 5 bubbles, and 7 bubbles were modelled in the pressboards to simulate aging over 8 d, 16 d, 32 d, and 48 d, respectively.

Figure 10 shows that the electric field intensity inside of the bubble and in its surroundings was notably higher than that near the pressboard. The intensity of the electric field increased by between 0.7 kV/mm and 1.5 kV/mm when the models with added bubbles were compared with those without bubbles.

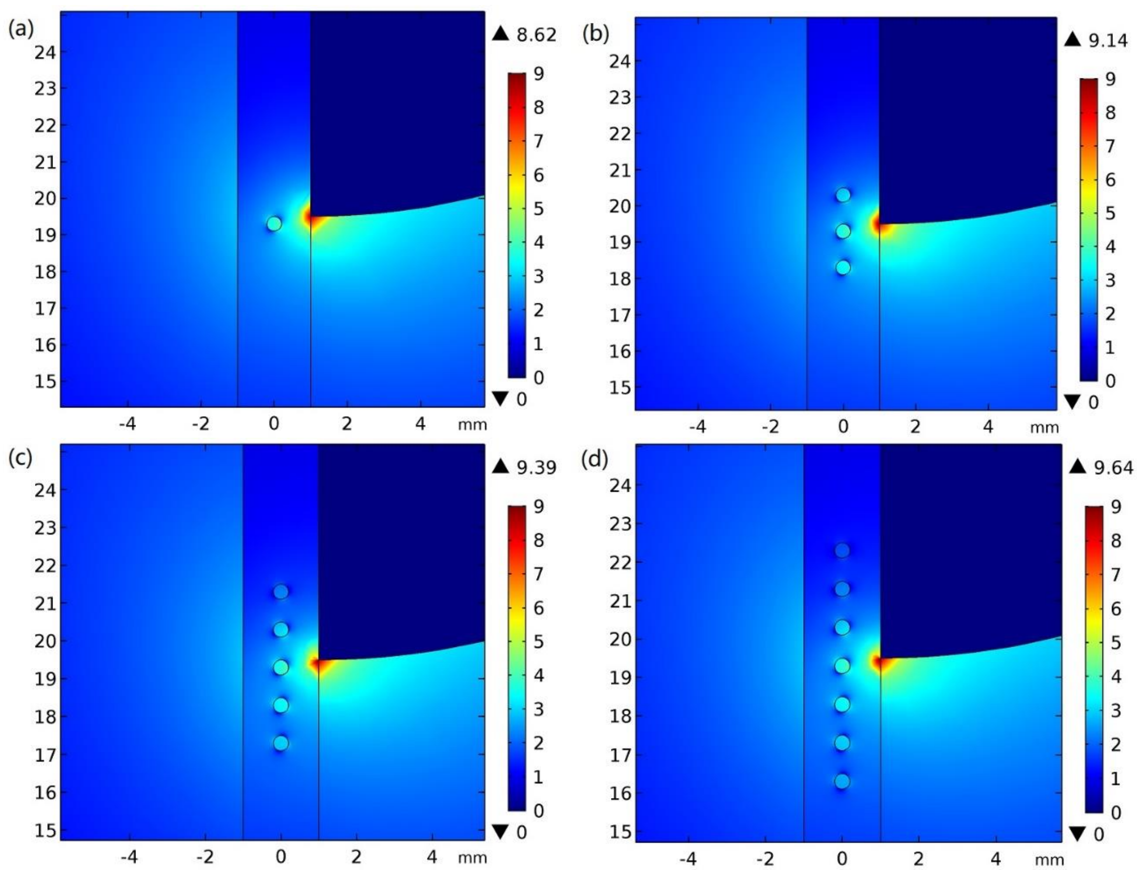


**Fig. 10.** Electric field nephogram for different cardboard ages: (a) 1 bubble; (b) 3 bubbles; (c) 5 bubbles; and (d) 7 bubbles

With an increase in the number of bubbles, the electric field intensity around the bubble increased remarkably. Local areas of high field intensity were remarkably increased both in the extent and magnitude of the field intensity, and the overall strength of the electric field on the pressboard was improved. Therefore, with an increase in the aging of the pressboard, the high-intensity field area was noticeably increased and the bubbles in the pressboard further promoted the development of discharge.

According to the experimental results and simulation analysis, aging mainly affects the development and later stage of the discharge from the pressboard. As the age increased, the total discharge magnitude did as well. When the PD amplitude was greater, then the number of discharge times was higher, the initial PD and flashover voltage of the pressboard were lower, and the PD development was faster.

## Microscopic Characteristics

To study the influence of the aging degree on the morphology of the pressboard, SEM was used to scan the samples of the pressboard with different aging degrees.

Figure 11 shows the SEM images of the pressboard without aging and after aging for 8 d, 32 d, and 48 d. The fibres of the untreated pressboard were relatively smooth and basically not broken. The fibres of the pressboard after aging for 8 d were deformed and had a small number of holes. Figure 11c shows that after aging for 32 d, the surface of the fibres was uneven. Compared with Fig. 11b, the holes were more obvious, there were many breaks in the fibre, and the fibre width was reduced notably. After 48 d of aging, the fibres tended to tear in some areas, the edges of the fibres were rough, and the mechanical strength of the fibres decreased.

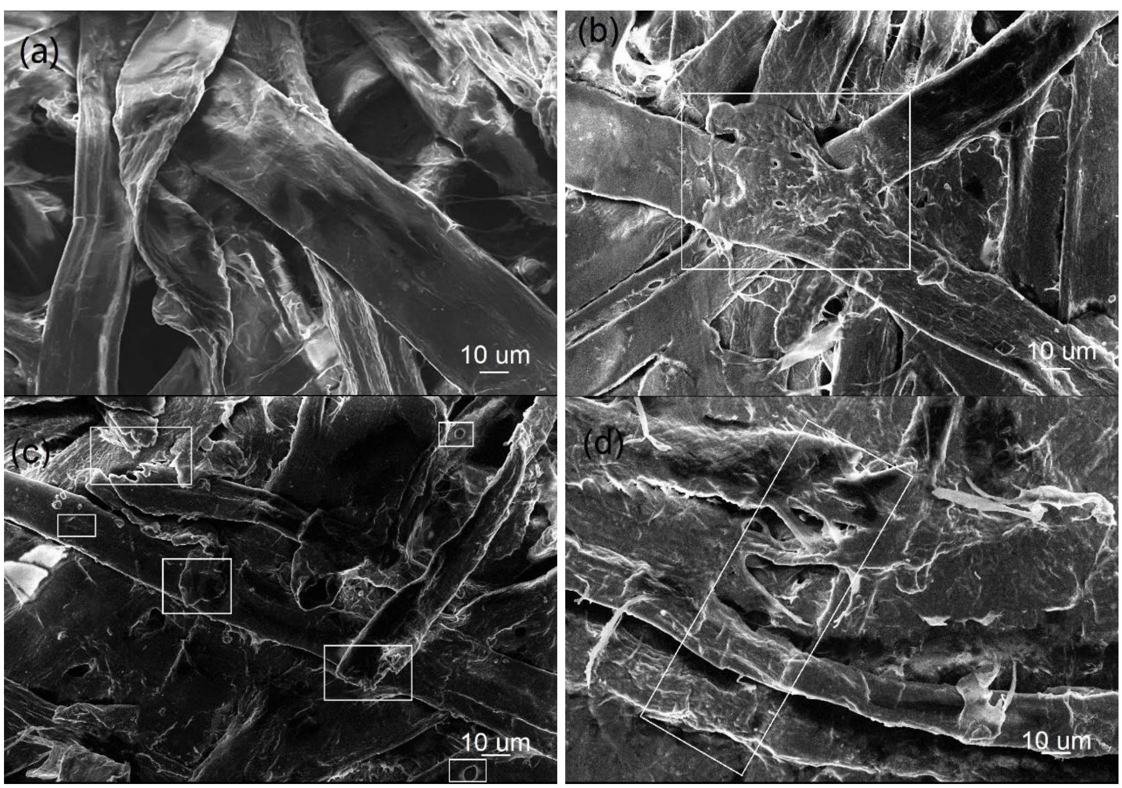


**Fig. 11.** SEM images of the pressboard with different aging times: (a) untreated pressboard, (b) aged for 8 d, (c) aged for 32 d, and (d) aged for 48 d

Figure 11 compares the thermal aging of the pressboard, which resulted in damage of the fibres. As the aging time increased, the flatness of the fibre surface became worse, the number and volume of the holes increased, and the compactness of the pressboard decreased. The aging of the pressboard also resulted in a smaller fibre width, breakage, and tear defects in some areas. The insulation and mechanical strength of the pressboard were reduced with the aging degree. Therefore, the discharge and flashover voltage of the pressboard decreased with the aging degree.

Figures 11d and 12 show that most of the fibres at the flashover point of the pressboard were broken after flashover. The fibre width was reduced, the holes were obvious, and the fibre surface was quite rough. According to the analysis, PD seriously damaged the surface morphology of the fibre, reduced the compactness of the fibre, and destroyed the insulation performance of the pressboard, which led to a more intense PD. Therefore, in the development and later PD stage, the pressboard PD was more intense with a longer aging time.

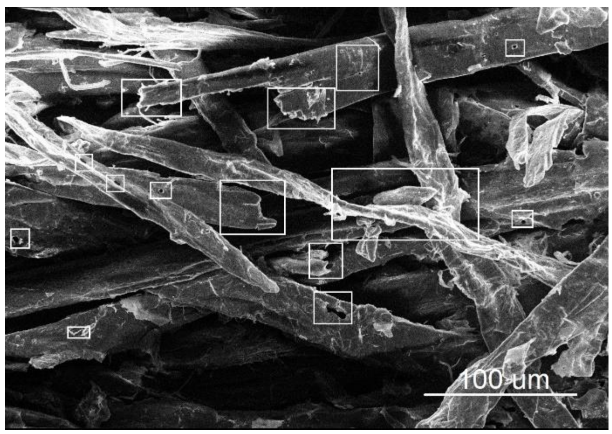


**Fig. 12.** SEM image of the pressboard after flashover

## Analysis of the FTIR Spectra

The FTIR spectra of the pressboards with different aging degrees before and after flashover are shown in Figs. 13a and 13b, respectively. According to the location of the absorption peaks of the chemical groups and their corresponding infrared spectra (Liao *et al.* 2011; Sarathi *et al.* 2014), it was seen that the variation in the chemical groups on the pressboard surface was as follows. The absorption peak located between 2200 $cm^{-1}$ and 2400 $cm^{-1}$ represents $CO_2$, which is the error of background during the experiment.

Two absorption peaks appeared between 2800 $cm^{-1}$ and 3000 $cm^{-1}$, which represented C-H chemical groups. In the figure, the absorption peak at 2850 $cm^{-1}$ represented a methine group, and the absorption peak at 2928 $cm^{-1}$ represented a methylene group. With an increased aging, the absorbance of the peaks decreased slightly and the decrease was not obvious. This indicated that the chemical group may have been damaged by thermal aging of the pressboard and the number of chemical groups was reduced.

The absorption peak between 3200 $cm^{-1}$ and 3500 $cm^{-1}$ was mainly caused by the presence of a fibrous hydroxyl group. Hydrogen atoms on hydroxyl groups may form hydrogen bonds with similar oxygen atoms. According to the spectra in Fig. 13, the absorbance of hydroxyl groups by the pressboards with high aging degrees decreased. This indicated that the hydrogen bonds between or inside the cellulose molecules broke down under the effect of aging, which led to a decrease in the number of hydrogen bonds. At the same time, the intermolecular force and mechanical properties of the insulation pressboard decreased.

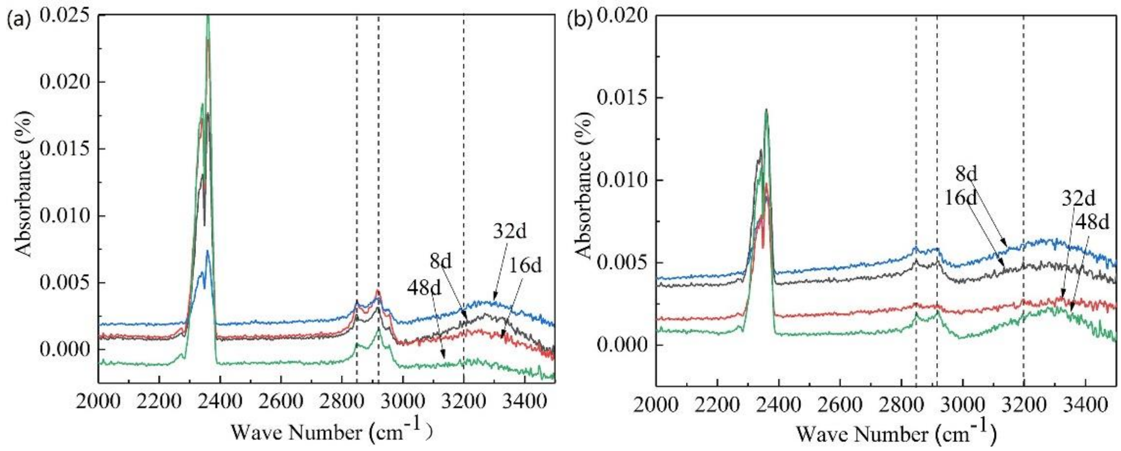


**Fig. 13.** FTIR spectra of the (a) pressboard before the experiment and (b) pressboard after flashover

## CONCLUSIONS

1. A hemispherical electrode was used to simulate the structure of a shielding electrode at the end of a bushing. It was found that the initial PD voltage and flashover voltage of the pressboard at the end of the bushing were both related to the aging degree. These voltages of the aged pressboard decreased slightly.
2. Based on the experiment on the hemispherical model, the effect of aging the pressboard at the end of the bushing on its PD was as follows. In the initial PD stage, the aging of the pressboard exerted little influence on the PD characteristics. With the development of PD, bubbles overflowed and became attached to the surface of the pressboard. These bubbles exerted an important influence on the electric field in the hemispherical models. The aging degree mainly affected the PD development and the subsequent stages affected the pressboard. With increased aging, the total discharge magnitude increased, the maximum discharge magnitude increased, the number of discharge times increased, and the PD development became more rapid.
3. The microscopic results indicated that thermal aging and PD destroyed the surface morphology of the fibre in the pressboard. When the aging time was longer, the damage to the fibre morphology was more serious. Aging of the pressboards destroyed the fibre flatness, reduced the fibre width, and decreased the compactness. With an increased aging time, the number of holes in the fibres increased, and there was more fibre breakage, and even tears, resulting in a decrease in the mechanical properties and insulation strength of the pressboard.
4. From the electric field simulation, it was found that when the aging time was longer, the electric field intensity areas in the pressboard was greater and PD was more likely to occur.
5. The thermal aging treatment caused changes to the internal structure of the pressboard, which changed the content of the relevant functional groups of the pressboard. The

hydroxyl group content decreased with aging of the insulating pressboard, so the intermolecular forces and mechanical properties of the insulation pressboard decreased. Therefore, the aging state of the insulating pressboard may be judged according to the functional group content.

## ACKNOWLEDGMENTS

This work was supported by "The Fundamental Research Funds for the Central Universities" (2016ZZD07).

## REFERENCES CITED

Chen, Q., Liu, H., Chi, M., Wang, Y., and Wei, X. (2017). "Experimental study on influence of trap parameters on dielectric characteristics of nano-modified insulation pressboard," *Materials* 10(1), 90. DOI: 10.3390/ma10010090

Cui, Y., Zhu, L., Ji, S., Cao, P., and Zhang, F. (2017). "Partial discharge development in needle-plane configuration of oil-paper insulation under AC voltage," *IEEE T. Dielect. El. In.* 24(4), 2469-2476. DOI: 10.1109/TDEI.2017.006270

Fofana, I., Wasserberg, V., Borsi, H. and Gockenbach, E. (2002). "Challenge of mixed insulating liquids for use in high-voltage transformers. II. Investigations of mix liquid impregnated paper insulation," *IEEE Electr. Insul. Mag.* 18(3), 18-31. DIO: 10.1109/MEI.2002.1014964

Hao, J., Liu, C., Li, Y., Liao, R., Liao, Q., and Tang, C. (2018). "Preparation nano-structure polytetrafluoroethylene (PTFE) functional film on the cellulose insulation polymer and its effect on the breakdown voltage and hydrophobicity properties," *Materials* 11(5), 851. DOI: 10.3390/ma11050851

Harbaji, M., Shaban, K., and El-Hag, A. (2015). "Classification of common partial discharge types in oil-paper insulation system using acoustic signals," *IEEE T. Dielect. El. In.* 22(3), 1674-1683. DOI: 10.1109/TDEI.2015.7116364

Liao, R.-j, Tang, C., Yang, L. -j, Feng, Y., and Sun, C.-x (2009). "'Influence of the copper ion on aging rate of oil-paper insulation in a power transformer," *IET Electric Power Application* 3(5), 407-412. DIO: 10.1049/iet-epa.2008.0159

Liao, R.-j., Zhou, X., Yang, L.-j., and Xiang, B. (2011). "The mid-infrared spectra characteristic of the transformer oil-paper insulation in thermal ageing process," *Journal of Chongqing University* 34, 1-6.

Li, J., Si, W., Yao, X., and Li, Y. (2009). "Partial discharge characteristics over differently aged oil/pressboard interfaces," *IEEE T. Dielect. El. In.* 16(6), 1640-1647. DOI: 10.1109/TDEI.2009.5361584

Mitchinson, P. M., Lewin, P. L., Chen, G., and Jarman, P. N. (2008). "A new approach to the study of surface discharge on the oil-pressboard interface," in: *IEEE International Conference on Dielectric Liquids*, Chasseneuil, France.

Munajad, A., Subroto, C., and Suwarno (2018). "Fourier transform infrared (FTIR) spectroscopy analysis of transformer paper in mineral oil-paper composite insulation under accelerated thermal aging," *Energies* 11(2), 364. DOI: 10.3390/en11020364

Sarathi, R., Merin Sheema, I., and Sundara Rajan, J. (2014). "Understanding surface discharge activity in copper sulphide diffused oil impregnated pressboard under AC voltages," *IEEE T. Dielect. El. In.* 21(2), 674-682. DOI: 10.1109/TDEI.2013.004039

Sun, J., Li, X., Zhu, L., Ji, S., and Cui, Y. (2017). "Partial discharge of needle-plane defect in oil-paper insulation under AC and DC combined voltages: Developing processes and characteristics," *Energies* 10(11), 1759. DOI: 10.3390/en10111759

Tobazcon, R. (1994). "Prebreakdown phenomena in dielectric liquids," *IEEE T. Dielect. El. In.* 1(6), 1132-1147. DOI: 10.1109/94.368650

Tu, Y., Chen, J., Wang, S., and Wang, W. (2016). "Moisture migration in oil-impregnated film insulation under thermal ageing," *IEEE T. Dielect. El. In.* 23(2), 1135-1141. DOI: 10.1109/TDEI.2015.005406

Wang, Y., Xiao, K., Chen, B., and Li, Y. (2015). "Study of the impact of initial moisture content in oil impregnated insulation paper on thermal aging rate of condenser bushing," *Energies* 8(12), 14298-14310. DOI: 10.3390/en81212429

Wei, Y.-H., Mu, H.-B., Deng, J.-B., and Zhang, G.-J. (2016a). "Effect of space charge on breakdown characteristics of aged oil-paper insulation under DC voltage," *IEEE T. Dielect. El. In.* 23(5), 3143-3150. DOI: 10.1109/TDEI.2016.7736879

Wei, Y.-H., Mu, H.-B., Zhang, G.-J., and Chen, G. (2016b). "A study of oil-impregnated paper insulation aged with thermal-electrical stress: PD characteristics and trap parameters," *IEEE T. Dielect. El. In.* 23(6), 3411-3420. DOI: 10.1109/TDEI.2016.005749

Xia, G., and Wu, G. (2016). "Study on the impact of initial moisture contents on ageing characteristics of transformer oil-paper insulation," in: *IEEE International Conference on High Voltage Engineering and Application*, Chengdu, China.

Xie, B., Chen, W., Zhou, Q., Du J., and Cui, L. (2016a). "Partition of the development stage of air-gap discharge in oil-paper insulation based on wavelet packet energy entropy," *IEEE T. Dielect. El. In.* 23(2), 866-872. DOI: 10.1109/TDEI.2015.005430

Xie, J., Lv, F., Wang, Y., Li, M., Liu, X., and Wang, K. (2016b). "The influence of pressboard aging on oil-paper insulation surface discharge development law," *Electrical Measurement & Instrumentation* 53, 87-92.

Yang, L. J., Lin, Y. D., Liao, R. J., Zhao, X. T., Sun, W. D., and Zhang, Y. Y. (2016). "Effects of temperature and aging on furfural partitioning in the oil-paper system of power transformers," *IEEE T. Dielect. El. In.* 23(3), 1393-1401. DOI: 10.1109/TDEI.2015.005530

Zhang, S., Peng, Z., Hu, W., Liu, P., and Wang, H. (2012). "Optimization of shielding electrode for UHV oil-gas bushing with improved hybrid algorithm combining particle swarm optimization and back-propagation neural network," *High Voltage Engineering* 38(9), 2195-2204. DOI: 10.3969/j.issn.1003-6520.2012.09.008

Zhang, S., Yan, J., Li, D., Liu, P., Peng, Z., and Zhang, S. (2017). "Optimal design of shielding structure in ultra-high voltage GIS bushing using artificial fish-swarm algorithm," in: *1st International Conference on Electrical Materials and Power - Equipment*, Xi'an, China, pp. 57-60.

Zhou, L., Wang, D., Guo, L., Wang, L., Jiang, J., and Liao, W. (2017). "FDS analysis for multilayer insulation paper with different aging status in traction transformer of high-speed railway," *IEEE T. Dielect. El. In.* 24(5), 3236-3244. DIO: 10.1109/TDEI.2017.006547

Zhou, Y., Huang, M., Chen, W., Lu, L., Jin, F., and Huang, J. (2015). "Space charge behavior evolution with thermal aging of oil-paper insulation," *IEEE T. Dielect. El. In.* 22(3), 1381-1388. DOI: 10.1109/TDEI.2015.7116326

Zhou, Z.-j., Hu, T., Cheng, L., Tian, K., Yang, J., Wang, X., Fang, F.-x., Kong, H.-y., and Qian, H. (2016). "Comparative study on accelerated thermal ageing of vegetable insulating oil-paperboard and mineral oil-paperboard," *Advanced Material Science and Engineering* 47, 64-73. DOI: 10.1142/9789813141612_0009

Zou, J., Chen, W., Wan, F., Fan, Z., and Du, L. (2016). "Raman spectral characteristics of oil-paper insulation and its application to ageing stage assessment of oil-immersed transformers," *Energies* 9(11), 946. DOI: 10.3390/en9110946

Article submitted: September 14, 2018; Peer review completed: November 26, 2018; Revised version received: December 1, 2018; Accepted: December 15, 2018; Published: January 7, 2019.
DOI: 10.15376/biores.14.1.1303-1316